*microLife*, 2026, **7**, uqag020
https://doi.org/10.1093/femsml/uqag020
Published: 15 May 2026
**Research Article**

# Comparative proteome analyses of human natural killer cells from patients after allogeneic stem cell transplantation and healthy individuals challenged with *Aspergillus fumigatus*

**Jan Springer [1], Matthias Drobny[1], Linda Heilig[1], Sabrina Kraus[1], Olaf Kniemeyer [2], Thomas Krüger[2], Christian Olischer[1], Lydia Bussemer[1], Gianni Panagiotou [3,4], Axel A. Brakhage[2,4], Hermann Einsele[1], Sascha Schäuble [3,#], Jürgen Löffler[1,*,#]**

[1]Department of Internal Medicine, University Hospital Würzburg, 97080 Würzburg, Germany
[2]Department of Molecular and Applied Microbiology, Leibniz Institute for Natural Product Research and Infection Biology–Hans Knöll Institute (Leibniz-HKI), 07745 Jena, Germany
[3]Department of Microbiome Dynamics, Leibniz Institute for Natural Product Research and Infection Biology–Hans Knöll Institute (Leibniz-HKI), 07745 Jena, Germany
[4]Institute of Microbiology, Faculty of Biological Sciences, Friedrich Schiller University Jena, 07743 Jena, Germany
*Corresponding author. University Hospital Würzburg, Medical Hospital II, Haus C11, Josef Schneider Strasse 2, 97080 Würzburg, Germany. E-mail: Loeffler_j@ukw.de
[#]Shared last authors.
**Editor:** Carmen Buchrieser

## Abstract

**Natural killer (NK) cells contribute to the innate immune system and are pivotal for the defence against opportunistic pathogens, including fungi. *Aspergillus fumigatus*(AF), a filamentous mold, can cause invasive pulmonary aspergillosis in immunocompromised patients, e.g. in patients after allogeneic stem cell transplantation (alloSCT). In this pilot study, we challenged NK cell samples from alloSCT recipients collected 90, 120, and 180 days after transplantation and from healthy individuals with AF and characterize the proteome response differences. We identified 2259 differentially abundant proteins between the NK cell proteomes of alloSCT recipients and healthy individuals. Among these, 1118 proteins were differentially abundant at all time points and 1931 proteins specifically at day 180 post-alloSCT. Following stimulation of NK cells with AF, we found a profoundly different early proteome (day 90, *n*=1652 proteins), while at day 180, only 77 proteins remained significantly differentially abundant. We identified, among others, a major differentially abundant protein cluster related to IL27RA (including OAS, STAT1, and MX). Furthermore, for selected markers [granzyme A (GZMA), Neural Cell Adhesion Molecule 1 (NCAM1/CD56), perforin-1 (PRF1)], we confirmed our proteome data by flow cytometry in NK cells from an independent second patient and healthy individual cohort. In conclusion, we demonstrate the advantage of combining comprehensive proteomic profiling with targeted flow cytometry to investigate NK cell responses to AF. Our data analysis connects STAT1 with IL27RA as well as granzyme, IFNg, and NCAM1 activity, which may be exploited towards future therapeutics warranting confirmation in larger study cohorts.**

**Keywords** Proteome analyses, NK cells, allogeneic stem cell transplantation, *Aspergillus fumigatus,* immune reconstitution, fungal infection

## Introduction

The mold *Aspergillus fumigatus* is an opportunistic fungal pathogen that can induce life-threatening invasive pulmonary aspergillosis (IPA) in immunocompromised patients suffering from hematological malignancies or undergoing allogeneic stem cell transplantation (alloSCT) (Segal 2009). The development of IPA in alloSCT recipients results in mortality rates of up to 50% (Latge and Chamilos 2019) and poor prognosis concerning long-term survival rates (Salmeron et al. 2012, Denning 2024).

The immune response to *A. fumigatus* comprizes a complex interplay of various immune cell populations, including T and B cells and innate macrophages, dendritic cells, neutrophils, and natural killer cells (Singh and Paterson 2005). However, after alloSCT, patients experience substantial T and B cell depletion for up to 2 years until their immune system is fully reconstituted (Corre et al. 2010).

**Received:** 26 September 2025. **Revised:** 16 April 2026. **Accepted:** 29 April 2026

NK cells are innate immune cells that make up ∼10%–15% of peripheral blood mononuclear cells (PBMCs) in healthy persons (Campbell and Hasegawa 2013, Schmidt et al. 2017). Upon encountering cancer cells, NK cells get activated and release their effector molecules granzyme A (GZMA) and perforin, which induce target cell lysis (Topham and Hewitt 2009). In addition, NK cells produce immune regulatory cytokines to stimulate and attract other immune cells while also exhibiting direct cytotoxicity against virus-infected cells by granule release (Robertson and Ritz 1990). Notably, the likelihood of developing IPA in patients undergoing alloSCT is significantly correlated with lower NK cell numbers and delayed NK cell reconstitution, according to a 12-month monitoring study (Stuehler et al. 2015).

Although it has been demonstrated that NK cells are essential to the host defence during an *A. fumigatus* infection, the underlying cellular pathomechanisms and their specific modes of action during the interaction with the fungus are still elusive (Qin et al. 2023). In this pilot study, we characterize the hitherto unknown proteome patterns of NK cells from alloSCT recipients, a group of patients with a high risk to be affected by IPA, in comparison to healthy individuals. To identify potential pathogen-driven differences in the proteome content of NK cells from allograft recipients and healthy individuals, a proteome comparison was also performed after *A. fumigatus in vitro* stimulation of NK cells from both populations. Our data show specific, differentially abundant proteins in NK cells when stimulated with fungi in comparison to unstimulated samples with a pronounced immune-regulatory component. Furthermore, selected proteins were confirmed in an independent group of allograft recipients and healthy individuals by flow cytometry, highlighting the robustness of the fungus-associated differences in protein profiles and the potential herein for developing alternative treatment options for immunocompromised patients.

# Materials and methods

## Patient information

Primary NK cells from eight adult patients undergoing alloSCT were included in this study. Detailed patient characteristics are displayed in Supplementary Table S1. The majority of patients suffered from acute leukemia (7/8) and, five out of eight received myeloablative conditioning. GvHD prophylaxis, including anti-thymocyte globulin administration and antimicrobial prophylaxis, was comparable across patients. No patient relapsed during the study period. Four of the eight patients developed acute GvHD, which did not exceed grade II. Importantly, no patient required systemic corticosteroid therapy for GvHD management. Thus, the observed findings appear to be independent of concomitant steroid exposure or other patient-specific factors.

Peripheral EDTA-anticoagulated blood (30 ml) was collected from patients at days 90, 120, and 180 after alloSCT. These time points were chosen to capture distinct phases of post-transplant immune reconstitution, including an early, intermediate, and late phase after transplantation, thereby assessing how the NK-cell proteomic landscape evolves over time in the clinically relevant period of heightened susceptibility to IPA. Furthermore, NK cells were isolated from the blood of healthy volunteers at a single time point and served as comparator cells.

## NK cell culture

NK cell isolation was performed using the MACSxpress R Whole Blood NK Cell Isolation Kit (negative isolation, Miltenyi Biotec). NK cells were cryopreserved in FCS/DMSO (90%/10%) in liquid nitrogen. Thawing of NK cells was performed using RPMI 1640 + 10% FCS pre-warmed to 37°C. Viability and cell number were determined using a VICELL XR cell counter (Beckmann Coulter) confirming consistent viabilities of at least 83% after thawing. NK cells were pre-stimulated with interleukin-2 (IL-2, 1000 IU/ml, Proleukin$^{TM}$, Novartis) overnight, plated at a cell density of $1 \times 10^6$ cells/ml.

For fungal co-cultures, NK cells ($1 \times 10^6$ cells/ml) were confronted with *A. fumigatus* germ tubes (MOI 0.5) or fresh RPMI 1640 + 10% FCS as control. After 6 h of co-culture, cells were harvested, centrifuged (300 *g*, 10 min), and further processed either by digestion (for subsequent proteome analysis) or processed for flow cytometry analysis (validation experiments).

## Culture of *A. fumigatus*

To generate *A. fumigatus* germ tubes, conidia (strain ATCC 46645; $10^6$/ml) were incubated overnight in RPMI 1640 while constantly shaking (200 rpm) at 25°C. Then, germ tubes were centrifuged (5000 *g*, 10 min) and resuspended in fresh medium including 10% FCS.

## In-solution digest

Each sample was washed with phosphate-buffered saline three times (300 *g*, 10 min). For cell lysis, 40 µl of trifluoroacetic acid (TFA) was added to the cells and incubated for 10 min at room temperature. Neutralization was performed with 400 µl 2 M Tris (12.1 *g*/50 ml). Subsequently, cysteine thiols were reduced and carbamidomethylated in one step for 30 min at 70°C by addition of 8.8 µl each of 500 mM TCEP (tris(2-carboxyethyl)phosphine) and 625 mM 2-chloroacetamide (CAA) both solved in 100 mM TEAB (triethylammonium bicarbonate). After spectrophotometric quantification (NanoDrop 1000, Peqlab) the same amount of protein was adjusted for each sample. Each sample was filled up with 100 mM Tris to gain a total volume of 450 µl and then the volume was divided into three tubes (150 µl aliquots) and the samples were diluted with 900 µl ultrapure water. Samples were digested for 18 h at 37°C after addition of Trypsin/Lys-C mix (Promega) at a protease-to-protein ratio of 1:10. Subsequently, the aliquots were reunited, and 40 µl TFA was added to set the pH to ∼2. Samples were desalted by peptide enrichment on C18 Spin Tips (Thermo HyperSep C18). Tryptic peptides were eluted with 200 µl of 0.1% TFA in 80/20 ACN/$H_2O$ and the solvent was evaporated by vacuum concentration. Dried peptides were resolubilized in 30 µl of 0.05% TFA in $H_2O$/ACN 98/2 (v/v) filtered through 10 kDa MWCO PES membrane spin filters (VWR). The filtrate was transferred to HPLC vials and injected into the liquid chromatography–tandem mass spectrometry (LC–MS/MS) instrument.

## LC–MS/MS analysis

Each sample was measured in triplicate (three analytical replicates). LC–MS/MS analysis was performed on an Ultimate 3000 nano RSLC system connected to an Orbitrap Exploris 480 mass

spectrometer (both Thermo Fisher Scientific, Waltham, MA, USA) with FAIMS. Peptide trapping for 5 min on an Acclaim Pep Map 100 column (2 cm x 75 μm, 3 μm) at 5 μl/min was followed by separation on an analytical Acclaim Pep Map RSLC nano column (50 cm x 75 μm, 2 μm). Mobile phase gradient elution of eluent A (0.1% (v/v) formic acid in water) mixed with eluent B (0.1% (v/v) formic acid in 90/10 acetonitrile/water) was performed using the following gradient: 0–5 min at 4% B, 30 min at 7% B, 60 min at 10% B, 100 min at 15% B, 140 min at 25% B, 180 min at 45% B, 200 min at 65% B, 210–215 min at 96% B, 215.1–240 min at 4% B. Positively charged ions were generated at a spray voltage of 2.2 kV using a stainless steel emitter attached to the Nanospray Flex Ion Source (Thermo Fisher Scientific). The quadrupole/orbitrap instrument was operated in full MS/data-dependent MS2 mode. Precursor ions were monitored at $m/z$ 300–1500 at a resolution of 120 000 FWHM (full width at half maximum) using a maximum injection time (ITmax) of 50 ms and 300% normalized AGC (automatic gain control) target. Precursor ions with a charge state of $z$=2–5 were filtered at an isolation width of $m/z$ 1.3 amu for further fragmentation at 28% HCD collision energy. MS2 ions were scanned at 15 000 FWHM (ITmax=40 ms, AGC= 200%). Four different compensation voltages were applied (−45 V, −60 V, −75 V, −90 V) .

## Protein database search

Tandem mass spectra were searched against the UniProt databases (2022/05/20) of *Homo sapiens* (https://www.uniprot.org/proteomes/UP000005640) and *A. Fumigatus* (https://www.uniprot.org/proteomes/UP000002530) using Proteome Discoverer (PD2.4, Thermo) and the database search algorithms Mascot 2.8, MS Fragger 3.4, MS Amanda 2.0, Sequest HT, and MSPepSearch (spectral library from NIST, human_hcd) with Precursor Detector node. Two missed cleavages were allowed for the tryptic digestion. The precursor mass tolerance was set to 10 ppm, and the fragment mass tolerance was set to 0.02 Da. Modifications were defined as dynamic Met oxidation, phosphorylation of Ser, Thr, and Tyr, protein N-term acetylation with and without Met-loss as well as static Cys carbamidomethylation. A strict false discovery rate (FDR) <1% (peptide and protein level) and search engine scores for Mascot >30 or MS Fragger >8 or MS Amanda >300 or Xcorr >4 was required for positive protein hits. The Percolator node of PD2.4 and a reverse decoy database was used for q-value validation of spectral matches. Only rank 1 proteins and peptides of the top scored proteins were counted. Label-free protein quantification was based on the Minora algorithm of PD2.4 using the precursor abundance based on intensity and a signal-to-noise ratio >5. Normalization was performed by using the total peptide amount method. Imputation of missing quan values was applied by using abundance values of 75% of the lowest abundance identified per sample. For the reference proteome analysis used for master protein abundance correction of the phosphoproteome data.

## Flow cytometry

NK cells were harvested, washed (10 min at 300 *g*), and extracellularly stained with anti- NCAM1/CD56 FITC, anti-CD3 APC Vio770 along with the fixable Viobility™ Live/Dead Dye (all Miltenyi Biotec). To evaluate expression of perforin (anti-PRF1 Viogreen, Miltenyi Biotec) and granzyme A (anti-GZMA APC, Miltenyi Biotec) intracellular staining was performed according to the Inside Stain Kit protocol (Miltenyi Biotec). Flow cytometric data was acquired on a CytoFLEX (Beckman Coulter Life Sciences) and analyzed using Kaluza v2.1 software (Beckman Coulter Life Sciences). Isolated NK cells were selected according to their forward and side scattering and single cells were gated based on SSC-A and SSC-H properties. Dead cells were excluded by live/dead staining. NK cells were identified as CD3 negative (CD3−). Among CD3− cells (NK cells), mean fluorescence intensities (MFIs) for the cell surface marker CD56 and the intracellular markers PRF1 and GZMA were determined. MFI of an unstained sample was defined as background and subtracted from the MFI of the corresponding stained sample.

## Analysis of abundance profiles

Statistical testing was performed by running a two tailed *t*-test and, when possible, with paired data to account for donor specific variation (e.g. stimulation of the same patient data with or without *A. fumigatus* infection).

Of note in the proteomics dataset NCAM1 was mapped to two different variants, H7BYX6 and A0A087WTF6, of which the latter was discarded, as it was no longer annotated (since release 2024_01/2024_01)**.** This was not necessary for FACS data analysis, where all abundance data were associated with NCAM1.

For time-point independent data assessment, alloSCT recipient data of all three time points were merged, while for time-point dependent analysis, each factor was grouped for each time-point individually. Again, two-tailed *t*-test statistics were computed for the different groups. All derived *P*-values were multiple-test corrected using *P*-value adjustment by Benjamini–Hochberg. Enrichment analysis was accomplished using the R package gprofiler2 (v0.2.3), which marks key driver ontology terms in the “highlighted” column. To exclude broad and less informative ontology terms, enriched categories were also filtered for background size $n \leq 150$ and an intersection size of $n \geq 3$ with the protein search query. Statistical analysis was performed using R (v4.3.0) and the package rstatix (v0.7.2). Convergence analysis of abundance profiles in alloSCT recipients over time was accomplished by first averaging abundance information and determining the absolute differences per time point. Subsequently, all absolute differences were normalized by dividing by the first time point absolute difference, followed by strict filtering for proteins that showed a consistent reduction in absolute abundance difference to healthy individuals (HD) over time.

# Results

## Proteome analysis of NK cells from healthy individuals and alloSCT recipient

At first we sought to delineate longitudinal changes in the proteomic profiles of alloSCT patients in comparison with healthy controls and to assess whether these alterations were accompanied by differences in the anti-*Aspergillus* response. To this end, NK cells collected at days 90, 120, and 180 post-alloSCT, alongside NK cells from healthy donors, were confronted with *A. fumigatus* or left untreated. A general workflow of the study is described in Fig. 1A. After LC–MS/MS analyses we were able to identify

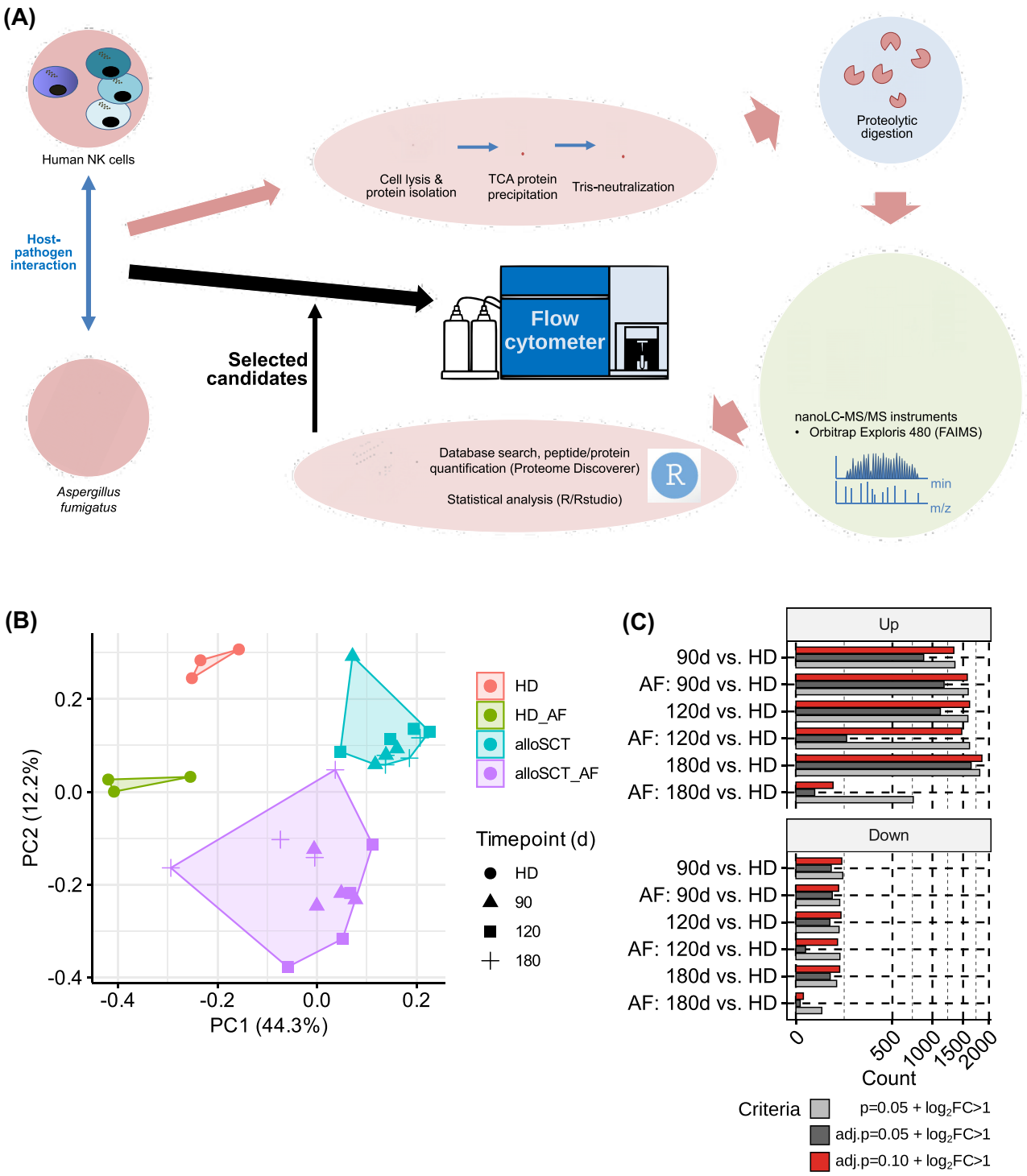


**Figure 1** Analysis approach of proteome data for *A. fumigatus* infection of human NK cells. (A) Workflow from acquisition of NK cell proteome data challenged with AF or not, to statistical analysis and flow cytometer validation experiments. (B) A principal component analysis of samples taken from patients at three different time points after alloSCT (days 90, 120, and 180) and from healthy individuals (HD) challenged with vs. without *A. fumigatus*.(C) Evaluation of statistical rigidity. Six pairwise comparisons divided into up- or down-regulated proteins were conducted and different thresholds evaluated.

5791 human proteins (Supplementary Table S2). A principal component analysis revealed clear separation of samples by group, distinguishing alloSCT recipients at days 90, 120, and 180 post-transplant from healthy individuals (HD) and further segregating samples by *A. Fumigatus* stimulation status (Fig. 1B). We analyzed different thresholds for statistical testing of six pairwise comparisons including tests for individual time point differences vs. HD abundance profiles either with or without *A. fumigatus* stimulation (Fig. 1C). Given the expected heterogeneity across the donors of our pilot study, an appropriate cut-off for statistical significance

had to be determined. To enable reasonable data exploration, to filter for biologically plausible effects and to increase sensitivity while still controlling the FDR using the Benjamini–Hochberg procedure, see Methods), we opted for using a combination of multiple test-adjusted statistical significance by FDR ($P \leq 0.10$) and an absolute $\log_2$(fold-change) $\geq 1$ as basis for our subsequent analyses (Fig. 1C). Across six comparisons for alloSCT recipient derived vs. HD proteomes with or without *A. fumigatus* stimulation, we identified 8457 significant differences encompassing 2676 unique DAPs in total over all comparisons (min = 3, max = 1846, mean = 705, Fig. 1C, Supplementary Table S3). Of these, 89% (2395) were upregulated in alloSCT recipients, showcasing a massive immune regulatory response in alloSCT recipients.

By combining pairwise statistical test results, we first explored DAPs in alloSCT recipients compared to HD samples irrespective of the time point. We found 2259 DAPs in at least one time point showing a pronounced base difference between HD and alloSCT recipients with 49.5% ($n$=1118) time-point independent significant changes and 1931 DAPs that remain differentially abundant up to 180 days after alloSCT (Fig. 2A). When challenging samples with *A. fumigatus*, we identified 1934 DAPs (Fig. 2B). Interestingly, while we observed a large concordance between DAPs for the first two time points compared to HD samples, significance was mainly lost at time point 180 days (1554 DAPs at 120 days, but only 62 across all time points, and only 77 at 180 days). This low DAP number at 180 days may indicate an equalization in protein content between HD and patient NK cells after contact with *A. fumigatus*.

To identify potential differences in the functional characteristics of alloSCT and HD samples we further conducted molecular enrichment by overrepresentation analysis (Supplementary Table S3). For unstimulated samples, our analysis revealed a large number of significant Gene Ontology:Biological Process (GO:BP) and KEGG terms ($n$ =1605) with 67 GO: BP highlighted driver ontologies (Fig. 2C, Supplementary Table S3, Methods). These included a number of immune response specific terms, among others, "positive regulation of RIG-I signaling pathway", "negative regulation of NK cell mediated immunity", or "negative regulation of macrophage chemotaxis" showcasing a pronounced base difference in molecular function between alloSCT and HD samples. After fungal stimulation we identified in total 1445 significant differences for GO: BP and KEGG terms with 80 GO: BP driver terms (Fig. 2D, Supplementary Table S3). These included immune relevant terms like "negative regulation of innate immune response", "myeloid leukocyte cytokine production," and "T cell migration," but also further protein and heme metabolic processes like "heme O/B biosynthetic processes", and "RISC complex assembly", among others.

Of note, both enrichment sets showed independently of the fungal challenge a differential activity of the "interleukin-27-mediated signaling pathway". While in the unstimulated setup the four proteins IL27RA, STAT1, oligoadenylatsynthetase (OASL), and MX1) were differentially abundant, again IL27RA, STAT1, OASL, and in addition OAS2 showed significant differential expression after *A. fumigatus* stimulation (Supplementary Table S3). Given interaction network analysis with STRING, STAT1 is a central regulator of these proteins and connects between IL27RA and OAS family members, a group of proteins involved in the innate immune response to infections, which show robust abundance over time, indicating its high biological relevance (Fig. 2E, F).

We next investigated the temporal dynamics of DAP fold changes over time compared to HD into depth. As the reduction of significant stimulated factors at time-point 180 days suggested (Fig. 2B), DAPs generally showed less significance at this time-point. Interestingly, while we observed 1564 (81%) DAPs in both *A. fumigatus* stimulated and in non-stimulated results, 370 DAPs were specific in alloSCT recipients compared to HD after *A. fumigatus* infection (Fig. 2G). These, however, did not yield any specific enriched function, except for “negative regulation of NF-kappaB transcription factor activity” following overrepresentation analysis (data not shown).

Since we hypothesize that recovering alloSCT recipients gain a more HD resembling protein profile over time, we next sought out to identify proteins with consistent reduction in absolute protein abundance differences over time. Among the differentially abundant proteins after fungal stimulation, 496 were compatible and decreasing towards HD levels at varying degrees (Fig. 3A, Supplementary Table S4). Enrichment analysis of these DAPs showed 310 significant GO:BP and KEGG categories, of which 32 were significant (Supplementary Table S4). After filtering for specific GO:BP categories, a number of immune relevant functional categories remained, including regulation of CD4/CD25 T cell differentiation and “granzyme-mediated programmed cell death signaling pathway” (Fig. 3B). The involved proteins were mostly upregulated but not significant at time-point 180 days after fungal stimulation (Fig. 3C).

By bringing both GO: BP categories mentioned above together with the category "interleukin-27-mediated signaling pathway," we revealed a broad interconnection between these three terms, having again STAT1 and the cytotoxic molecules perforin and GZMA, K, and B and the degranulation marker LAMP1 in central roles (Fig. 3D). As pathways-independent factor NCAM1 was included into the network showing its strong relation to many of the intrinsic factors, This network comprizes direct interactions of NCAM1 with some major NK cell effector molecules, including the cytolytic repertoire of NK cells and the STAT1-dependent cytokine signalling including IL27 and IFN-$\gamma$ (Fig. 3D).

## Proteome validation by flow cytometry

Finally, to confirm our proteome data, we complemented our analysis by investigating selected proteins with flow cytometry as a methodological independent quantitative protein abundance analysis (Fig. 4; patients nos. 5–8, Supplementary Table S1). Candidates were selected using an educated guess strategy in combination with own pre-existing datasets. A comparison of proteomics with flow cytometry for GZMA, PRF1, and NCAM1 (Fig. 4) revealed concordant abundance profiles across all three markers validating our proteome findings. Briefly, while time point-independent analysis revealed weak or no significant reduction in HD, but significant abundance decrease in alloSCT recipients after *A. fumigatus* stimulation (Fig. 4A, B). The analysis of our data per time point showed a reduction after *A. fumigatus* stimulation in all three factors, again with significance only in the FACS data (Fig. 4C, D). This signifies that, while proteomics provided a holistic insight, independent analysis by FACS was substantially more robust and showed consistently improved statistics, underscoring the need for complementary follow-up analyses. Strikingly, especially in the time-resolved FACS data (Fig. 4D), we observed that GZMA, PRF1, and NCAM1 get back to HD resembling levels

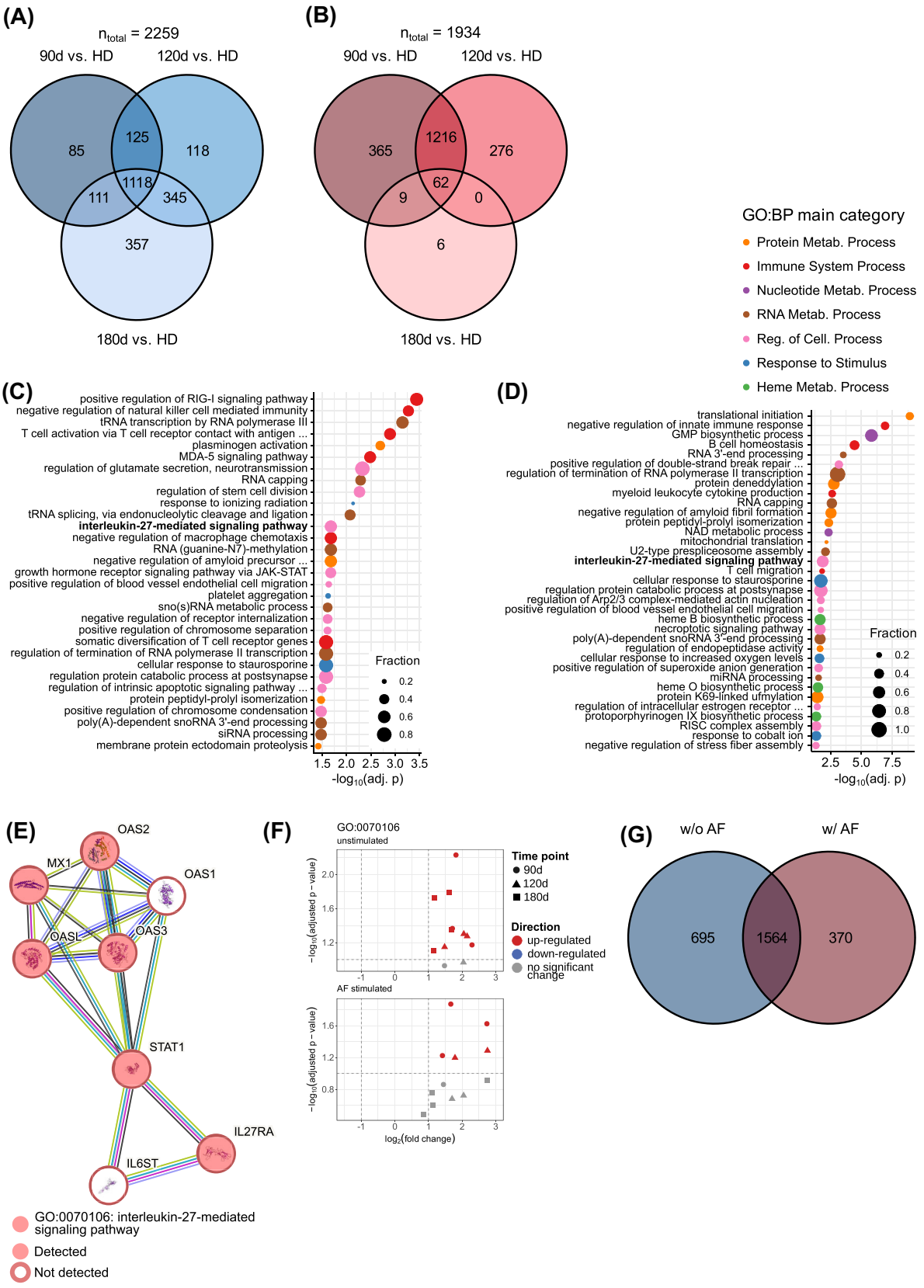


**Figure 2** Differentially abundant proteins (DAPs). (A–B) Venn diagrams showing intersections and time-point specific responses without (A) *A. fumigatus* (AF) and with (B) AF stimulation. (C–D) overrepresentation analysis results for driver terms of Gene Ontology: Biological Processes (Methods) present in NK cells in absence (C) and presence (D) of AF. Interaction network analysis using STRING (E) and detailed abundance pattern over time and by fold change/adjusted *P* value (F) of significantly differing proteins associated to the IL27-mediated signaling pathway (GO:0 070 106, bold in C–D). (G) AF-status differences of time-point independent DAPs.

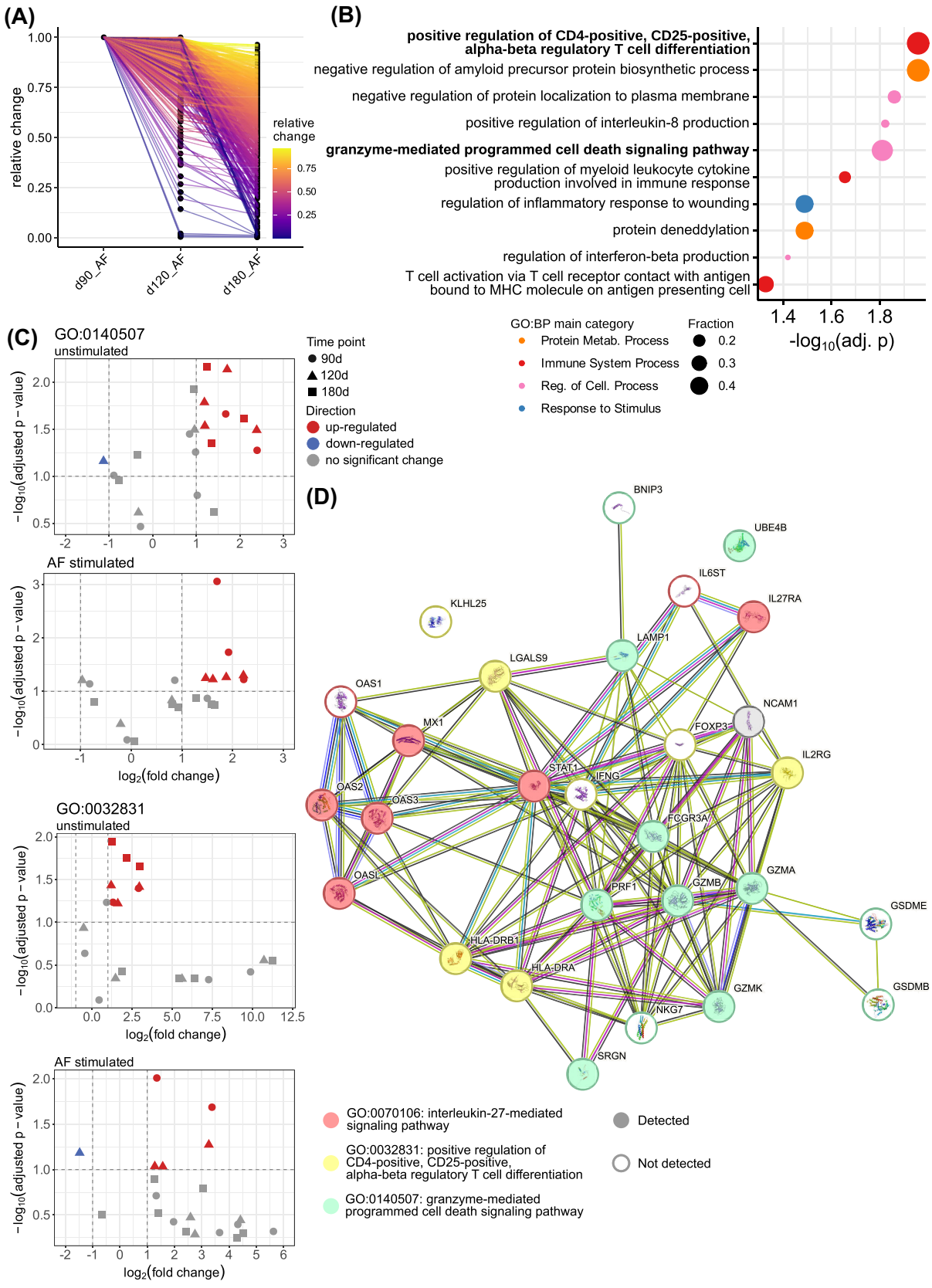


**Figure 3** DAPs after fungal stimulation (AF) filtered for strict decreasing over time. (A) Degree of decrease (days 90, 120, and 180) towards healthy control levels (Supplementary Table S4). (B) Enrichment analysis of DAPs showing significant Gene Ontology:Biological Process (GO:BP). (C) DAPs of selected immunorelevant functional categories (GO:0 140 507, granzyme-mediated programmed cell death signaling pathway; GO:0 032 831, positive regulation of CD4-positive, CD25-positive, alpha–beta regulatory T cell differentiation) ordered by stimulation condition and by fold change/adjusted *P* value. (D) Interaction network analysis of three selected immunoregulatory enriched categories in context of NCAM1 interaction using STRING.

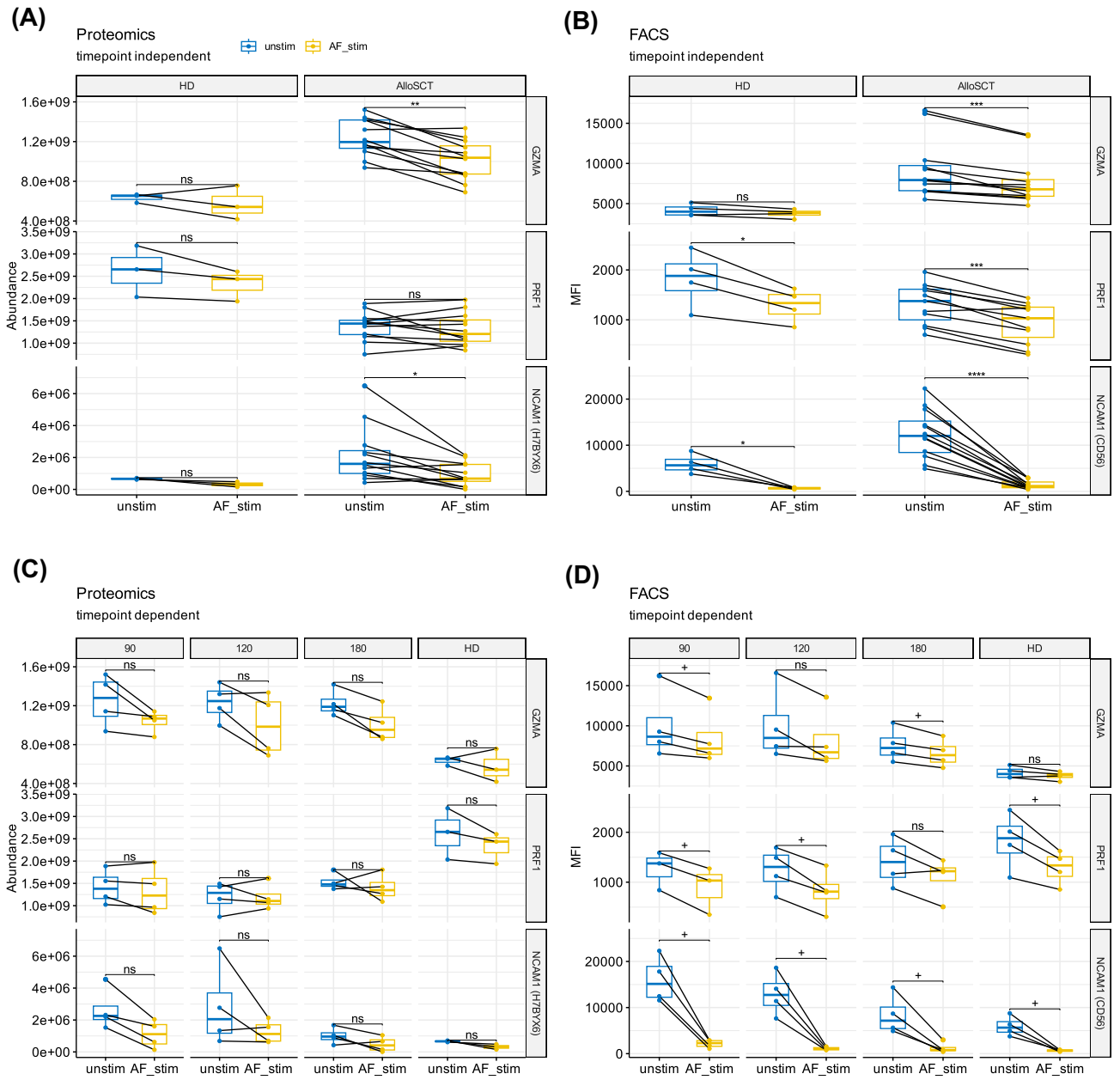


**Figure 4** Proteome validation by methodological independent quantitative protein abundance analysis (fluorescence cytometry, FACS). (A–B) Time-point-independent analysis of selected protein factors (GZMA/granzyme A, PRF1, perforin, and NCAM1/CD56) comparing proteome (A) and FACS (B) data. (C–D) Time point resolved abundance and statistical analysis comparing proteome (C) and FACS (D) data. Adjusted *P* according to two tailed *t*-test statistics: ∗∗∗∗: $P \leq$1e-4, ∗∗∗: $P \leq 0.001$, ∗∗: $P \leq 0.01$, ∗: $P \leq 0.05$, +: $P \leq 0.1$, ns: not significant. Unstim: unstimulated data. AF_stim: *A. fumigatus* stimulated data. MFI: mean fluorescence intensities

over time, both in unstimulated and in *A. fumigatus* stimulated data with high reproducibility. Whereas time-point-independent data showed a significant decrease after *A. fumigatus* stimulation in alloSCT recipients ($P \leq 0.001$), which was less pronounced in HD ($P \leq 0.05$ for PRF1 and NCAM1, and not significant for GZMA, Fig. 4B), time point-resolved data showed significant decrease in at least two time points in alloSCT recipients ($P \leq 0.1$) and in HD ($P \leq 0.1$, except for GZMA, Fig. 4D). In summary, our data suggest that in the course of an alloSCT, expression of a selection of NK cell-relevant functional proteins becomes similar to that of HD. This was particularly evident in connection with the stimulation of NK cells with *A. fumigatus*, whereas the composition in unstimulated cells was still quite different between HD and recipients of an allograft.

## Discussion

The proteome composition of human NK cells interacting with *A. fumigatus* is so far unknown and most proteomic study on NK cells focused on their antiviral response (Bi et al. 2023). However, knowledge about specific DAPs can give important insights in the biological function of NK cells during their defence against pathogens, including molds. Furthermore, and of particular rele-

vance are DAPs from NK cells isolated from patients receiving an allograft. Such patients are frequently affected by IPA, which implies potential immune cell functional deficiencies compared to intact immune responses observed in healthy individuals. To our knowledge for the first time, we here compared the proteome patterns of primary NK cells collected from randomly selected recipients of an allograft at defined time points post-transplant and from HD. In addition, the study aimed to explore differences in the NK cell proteomes between alloSCT samples and HD samples stimulated *in vitro* with the fungal pathogen *A. fumigatus.* Our data analysis was conducted in an exploratory manner, identifying a broad range of dynamically regulated molecular functions, which we summarized into principal protein signatures. From these, we distilled selected key proteins that may serve as a basis for future, larger and more standardized studies. Notably, several DAPs—beyond those involved in IL-27 signaling—were also associated with pathways such as RIG-I signaling, host heme biosynthesis, and protein deneddylation, which merit further investigation in dedicated follow-up studies.

The collection of the patient samples followed the same longitudinal approach as previously described (Weiss et al. 2020). This allowed the monitoring of protein expression by proteomics and flow cytometry until six months after alloSCT. Interestingly, analysis of a broad range of clinical data revealed that there was no significant impact of the clinical variables tested, including different infectious complications (Supplementary Table 1). Four of the eight patients developed acute Graft versus Host Disease (GvHD), but not beyond grade II. Importantly, no patient required systemic corticosteroid therapy for GvHD management, a factor that could have directly influenced NK cell functionality (Luo et al. 2025). Noteworthy, patient no. 7 had a single positive galactomannan (GM) test in the Bronchoalveolar Lavage Fluid at day 6 after alloSCT, however, all additional GM tests as well as ß-glucan assays remained negative, including tests which were performed shortly around NK cell sampling (at days 70 and 99). Therefore, we assume that the positive GM test result, which was 84 days prior to the first NK cell collection, did not affect their antifungal efficacy.

NK cells are essential during fungal infections, which has been shown in mouse models as well as in clinical studies. As an example, Stuehler et al. (2015) monitored recipients of an allograft over 12 months and found a clear correlation between reduced NK cell counts and delayed NK cell reconstitution with a higher risk of developing invasive aspergillosis in patients receiving SCT (Stuehler et al. 2015). In a previous study, we collected peripheral blood from allograft recipients at defined time points after alloSCT (days 60, 90, 120, and 180). By using multiplex immunoassays, we were able to describe substantial immune dysfunctions in patient NK cells compared to NK cells from healthy individuals, which persisted until 180 days post-alloSCT (Weiss et al. 2020). However, the overall NK cell characteristics during confrontation with a fungal pathogen remained largely unknown. While next generation sequencing studies have shown that the transcriptomes of immune cells change over time and show characteristic gene expression patterns after stimulation with *A. fumigatus* (Seelbinder et al. 2020), the proteome patterns of human NK cells, stimulated with *A. fumigatus*, remained to be characterized.

Exploratory studies are conducted to identify key variables, generate hypotheses, and to establish the feasibility for larger studies. Our pilot study revealed large numbers of DAPs in the different settings. Even at day 180 after alloSCT, 1931 DAPs still existed between unstimulated NK cells isolated from patients and from HD, indicating that such differences in the protein composition might exist protractedly. In contrast, if NK cells from patients or HD are challenged with *A. fumigatus*, DAPs were numerous at earlier time points after transplantation only (until day 120), adapting the protein composition after 180 days, possibly indicating a functional approach of these NK cells to healthy individuals. However, we cannot rule out that the loss in significance at later time-points might be due to study size, patient heterogeneity and history, despite controlling for donor origin as co-factor in our statistical designs.

Among others, our proteome data sets revealed IL27RA as a major, differentially abundant protein (together with different others from this protein cluster, including OAS, STAT1, and MX, Figs. 2, 3). IL27RA builds up together with the gp130 subunit a functional receptor complex, which binds IL27 and which activates JAK1 and STAT1 signals. IL27 is a key player in the IL15/IL18-mediated activation of NK cells (Choi et al. 2019), and has both, pro- and anti- inflammatory properties. In general, IL27 is a potent T cell immune modulator, enhancing Th1 differentiation, antagonizing Th17 cells, and promoting Treg responses against *Aspergillus* (Thompson and Orr 2018). Recently, Strickland et al. 2022) were able to show that IL27 is required for growth inhibition of *A. fumigatus* in the lung. This increased growth of *A. fumigatus* in IL27RA $-/-$ mice was associated with reduced IL12, TNFa, and Tbet expression, as well as reduced CD4 cell counts in murine lungs (Strickland et al. 2022). While their work relies on defined murine models, our study investigates human NK cells derived from hematopoietic stem cell transplant recipients. This allows identifying a broader temporal proteomic program associated with NK-cell responsiveness to *A. fumigatus* across different stages after transplantation. Furthermore, our data revealed that IL-27A is linked to specific functional and molecular features of NK-cell antifungal activation in this patient population, thereby offering a more detailed mechanistic framework for understanding how NK-cell responses are shaped during immune reconstitution.

Furthermore, IL27 is able to sensitize NK cells to augment both *in vitro* and *in vivo* responses mediated via the *A. fumigatus* receptor NKG2D (Kumar et al. 2019, Charpak-Amikam et al. 2024). Notably, also STAT1, a major transcription factor in NK cells, showed statistically significant differences, a major transcription factor in NK cells. STAT1 regulates, among many other functions, the production of interferon-$\gamma$, which is a key player in the NK cell dependent activation of T cells and can restore immune function to certain extend in fungal sepsis patients (Delsing et al. 2014).

Finally, we complemented our proteome analysis by quantifying the abundancy of selected proteins (NCAM1, GZMA, PRF1) using flow cytometry, an alternative method that allows protein quantification independent from LC–MS based proteomics (Fig. 4). This comparative analysis was again carried out in the form of a time series. For NCAM1, we detected higher general abundances in patients after alloSCT compared to HD by both methods (especially at day 90, with a markedly higher level of NCAM1 abundance). Interestingly, levels of NCAM1 abundancy were comparable at day 180 between healthy individuals and allograft recipients. The observation that early after alloSCT, NK cells display a higher percentage of NCAM1$^{bright}$ cells is in agreement with our previous study results (Weiss et al. 2020) and could be confirmed in the current study (data not shown). After stimulation of NK cells with *A. fumigatus*,

we confirmed the reduction of NCAM1 abundancy in NK cells isolated from healthy individuals and alloSCT recipients, observed in our proteome data, with flow cytometry (independent of the time point). The fact that NCAM1 relocalizes partly to the immunological synapse after *A. fumigatus* GAG stimulation was shown previously for healthy individuals (Ziegler et al. 2017, Heilig et al. 2024). In addition to this receptor relocalization, it is well known that NCAM1 is party internalized and rapidly degraded in the NK cell cytoplasm (Santiago et al. 2018). Lastly, the predominantly found NCAM1$^{bright}$ phenotype early after alloSCT reflects relatively immature NK cells with little cytolytic activity but a high capacity to release cytokines. In consequence, these NK cells mainly contribute to the attraction of further immune cell populations, such as macrophages and PMN, immune cells which potentially might have immature phenotypes and limited immune functions as well. Complete matching with the phenotype of NK cells from HD appears to be achieved only 180 d after alloSCT.

Perforin-1 (PRF1) and granzyme A (GZMA) are both secreted after treatment of NK cells with *A. fumigatus* (Bouzani et al. 2011). In consequence, we hypothesize that reduced abundancies of both markers detected by FACS and proteomics are due to the fact that both markers were secreted subsequent to fungal NK cell stimulation and, in consequence, were not detectable by both methods after fungal challenge. This reduction was reproducibly observed in NK cells from allograft recipients as well as in healthy NK cells. Interestingly, PRF1 and GZMA abundances were similar between healthy individuals and allograft recipients already 180 days after alloSCT.

To assess whether the differential abundance of NCAM1, PRF1, and GZMA observed upon *A. fumigatus* stimulation is conserved across *Aspergillus* species, we performed an additional independent pilot study based on flow cytometry, using NK cells from healthy donors and alloSCT patients, stimulated with *A. flavus* and *A. terreus*, respectively. Stimulation of NK cells from both cohorts with both fungi largely recapitulated the *A. fumigatus*-associated reduction in NCAM1 abundance, while, unlike with *A. fumigatus*, PRF1 and GZMA levels remained largely unchanged across cohorts (data not shown). Together, these data support a model in which *Aspergillus* species differentially modulate NK cell phenotype. This is consistent with species-specific differences in fungal cell wall architecture and immune recognition, and may contribute to the distinct clinical behavior and immune evasion strategies described for different *Aspergillus* species (van de Veerdonk et al. 2008, Lass-Florl et al. 2021). However, given the pilot nature of this study, larger-scale investigations integrating proteome-wide analyses and systematic cross-species comparisons will be required to robustly define species-specific NK cell responses.

Despite the fact that this pilot study shows major limitations especially in the small sample size, we were able to obtain a large number of significant DAPs, which differed in stimulated and unstimulated NK cells as well as between allograft recipients and healthy individuals, respectively. In consequence, our study exemplifies the feasibility and meaningfulness of proteome analyses under the chosen experimental settings and samples and can serve as a basis for future large well-designed studies. While our proteomics data enabled us to characterize the NK cell immune response in alloSCT recipients from a macro-perspective, the subsequent flow cytometry was essential to provide reproducible insights into the time-resolved recovery of infection-relevant immune response, for particularly relevant, selected markers. Future studies have the potential to define promising NK cell candidate proteins for example as targets for immunotherapy and to identify specific biomarkers, which are relevant in the NK cell—*A. fumigatus* interplay, especially in early post-transplant patients.

## Acknowledgements

This study obtained written consent by the ethics committee of the University of Wuerzburg (#34/15).

## Supplementary material

Supplementary material is available at *FEMSML Journal* online.

## Conflicts of interest

None declared.

## Funding

The study was supported by the Deutsche Forschungsgemeinschaft (DFG) within the Collaborative Research Center CRC124 FungiNet "Pathogenic fungi and their human host: Networks of interaction," DFG project number 210879364 (project A2 to H.E. and J.L., Z2 to O.K., and INF to G.P. and S.S.). The funders had no role in study design, data collection and analysis, decision to publish, or preparation of the manuscript.

## Data availability

The mass spectrometry proteomics data have been deposited to the ProteomeXchange Consortium via the PRIDE (Perez-Riverol et al. 2025) partner repository with the dataset identifier PXD068702 and DOI: 10.6019/PXD068702.

## References

Bi W, Kraft A, Engelskircher S *et al.* Proteomics reveals a global phenotypic shift of NK cells in HCV patients treated with direct-acting antivirals. *Eur J Immunol* 2023;**53**:e2250291. https://doi.org/10.1002/eji.202250291.

Bouzani M, Ok M, McCormick A *et al.* Human NK cells display important antifungal activity against *Aspergillus fumigatus*, which is directly mediated by IFN-gamma release. *J Immunol* 2011;**187**:1369–76. https://doi.org/10.4049/jimmunol.1003593.

Campbell KS, Hasegawa J NK cell biology: an update and future directions. *J Allergy Clin Immunol* 2013;**132**:536–44. https://doi.org/10.1016/j.jaci.2013.07.006.

Charpak-Amikam Y, Kournos M, Kotzur R *et al.* The activating receptor NKG2D is an anti-fungal pattern recognition receptor. *Nat Commun* 2024;**15**:8664. https://doi.org/10.1038/s41467-024-52913-2.

Choi YH, Lim EJ, Kim SW *et al.* IL-27 enhances IL-15/IL-18-mediated activation of human natural killer cells. *J Immunother Cancer* 2019;**7**:168. https://doi.org/10.1186/s40425-019-0652-7.

Corre E, Carmagnat M, Busson M *et al.* Long-term immune deficiency after allogenic stem cell transplation: b-cell deficiency is associated with late infections. *Haematologica* 2010;**95**:1025–9. https://doi.org/10.3324/haematol.2009.018853.

Delsing CE, Gresnigt MS, Leentjens J *et al.* Interferon-gamma as adjunctive immunotherapy for invasive fungal infections: a case series. *BMC Infect Dis* 2014;**14**:166. https://doi.org/10.1186/1471-2334-14-166.

Denning DW. Global incidence and mortality of severe fungal disease. *Lancet Infect Dis* 2024;**24**:e428–38. https://doi.org/10.1016/S1473-3099(23)00692-8.

Heilig L, Natasha F, Trinks N *et al.* CD56-mediated activation of human natural killer cells is triggered by *Aspergillus fumigatus* galactosaminogalactan. *PLoS Pathog* 2024;**20**:e1012315. https://doi.org/10.1371/journal.ppat.1012315.

Kumar P, Rajasekaran K, Nanbakhsh A *et al.* IL-27 promotes NK cell effector functions via Maf-Nrf2 pathway during influenza infection. *Sci Rep* 2019;**9**:4984. https://doi.org/10.1038/s41598-019-41478-6.

Lass-Flörl C, Dietl A-M, Kontoyiannis DP *et al. Aspergillus* terreus species complex. *Clin Microbiol Rev* 2021;**34**:e0031120. https://doi.org/10.1128/CMR.00311-20.

Latgé J-P, Chamilos G. *Aspergillus fumigatus* and *Aspergillosis* in 2019. *Clin Microbiol Rev* 2019;**33**:e00140–18. https://doi.org/10.1128/CMR.00140-18.

Luo T, Zhou R, Sun Y. The impact of postoperative glucocorticoids on complications after head and neck cancer surgery with free flap reconstruction: a retrospective study. *PLoS One* 2025;**20**:e0319655. https://doi.org/10.1371/journal.pone.0319655.

Perez-Riverol Y, Bandla C, Kundu DJ *et al.* The PRIDE database at 20 years: 2025 update. *Nucleic Acids Res* 2025;**53**:D543–53. https://doi.org/10.1093/nar/gkae1011.

Qin R, Qin J, Li X *et al.* Influence of immunosuppressive drugs on natural killer cells in therapeutic drug exposure in liver transplantation. *Hepatobiliary surgery and nutrition* 2023;**12**:835–53. https://doi.org/10.21037/hbsn-22-438.

Robertson MJ, Ritz J. Biology and clinical relevance of human natural killer cells. *Blood* 1990;**76**:2421–38. https://doi.org/10.1182/blood.V76.12.2421.2421.

Salmeron G, Porcher R, Bergeron A *et al.* Persistent poor long-term prognosis of allogeneic hematopoietic stem cell transplant recipients surviving invasive aspergillosis. *Haematologica* 2012;**97**:1357–63. https://doi.org/10.3324/haematol.2011.058255.

Santiago V, Rezvani K, Sekine T *et al.* Human NK cells develop an exhaustion phenotype during polar degranulation at the *Aspergillus fumigatus* hyphal synapse. *Front Immunol* 2018;**9**:2344. https://doi.org/10.3389/fimmu.2018.02344.

Schmidt S, Tramsen L, Lehrnbecher T. Natural killer cells in antifungal immunity. *Front Immunol* 2017;**8**:1623. https://doi.org/10.3389/fimmu.2017.01623.

Seelbinder B, Wallstabe J, Marischen L *et al.* Triple RNA-seq reveals synergy in a human virus-fungus co-infection model. *Cell Rep* 2020;**33**:108389. https://doi.org/10.1016/j.celrep.2020.108389.

Segal BH. Aspergillosis. *N Engl J Med* 2009;**360**:1870–84. https://doi.org/10.1056/NEJMra0808853.

Singh N, Paterson DL. Aspergillus infections in transplant recipients. *Clin Microbiol Rev* 2005;**18**:44–69. https://doi.org/10.1128/CMR.18.1.44-69.2005.

Strickland AB, Sun D, Sun P *et al.* IL-27 signaling promotes Th1 responses and is required to inhibit fungal growth in the lung during repeated exposure to *Aspergillus fumigatus*. *ImmunoHorizons* 2022;**6**:78–89. https://doi.org/10.4049/immunohorizons.2100117.

Stuehler C, Kuenzli E, Jaeger VK *et al.* Immune reconstitution after allogeneic hematopoietic stem cell transplantation and association with occurrence and outcome of invasive *Aspergillosis*. *J Infect Dis* 2015;**212**:959–67. https://doi.org/10.1093/infdis/jiv143.

Thompson A, Orr SJ. Emerging IL-12 family cytokines in the fight against fungal infections. *Cytokine* 2018;**111**:398–407. https://doi.org/10.1016/j.cyto.2018.05.019.

Topham NJ, Hewitt EW. Natural killer cell cytotoxicity: how do they pull the trigger?. *Immunology* 2009;**128**:7–15. https://doi.org/10.1111/j.1365-2567.2009.03123.x.

van de Veerdonk FL, Kullberg BJ, van der Meer JW *et al.* Host-microbe interactions: innate pattern recognition of fungal pathogens. *Curr Opin Microbiol* 2008;**11**:305–12. https://doi.org/10.1016/j.mib.2008.06.002.

Weiss E, Schlegel J, Terpitz U *et al.* Reconstituting NK cells after alloSCT show impaired response to the fungal pathogen *Aspergillus fumigatus*. *Front Immunol* 2020;**11**:2117. https://doi.org/10.3389/fimmu.2020.02117.

Ziegler S, Weiss E, Schmitt A-L *et al.* CD56 is a pathogen recognition receptor on human natural killer cells. *Sci Rep* 2017;**7**:6138. https://doi.org/10.1038/s41598-017-06238-4.

**Received:** 26 September 2025. **Revised:** 16 April 2026. **Accepted:** 29 April 2026